



Effects of carbon nanotubes addition on the superconducting properties and critical current density of $\text{NdBa}_2\text{Cu}_3\text{O}_{7-\delta}$

Tet Vui Chong¹ · Shin King Loh¹ · Chiew Han Liow² · Roslan Abd-Shukor³

Received: 27 April 2022 / Accepted: 16 July 2022 / Published online: 4 August 2022
© The Author(s) 2022

Abstract

Polycrystalline $\text{NdBa}_2\text{Cu}_3\text{O}_{7-\delta}$ samples with 0 to 1.5 wt% carbon nanotubes (CNTs) addition have been synthesized via the solid-state reaction method. The samples were examined by the four-point probe temperature-dependent electrical resistance, critical current density and AC susceptibility measurements. X-ray diffraction (XRD) patterns showed that the addition of CNTs did not change the orthorhombic structure of the samples and there was no systematic variation in the lattice parameters. CNTs addition increased the transition temperature with the highest onset transition temperature, $T_{c \text{ onset}} = 96$ K for the 1 wt% added sample. The critical current density increased from 2600 mA/cm² for the pure $\text{NdBa}_2\text{Cu}_3\text{O}_{7-\delta}$ to 4960 mA/cm² for the 1.0 wt% CNTs added sample. It is suggested that the grain boundaries improved with CNTs addition, and this plays an important role in the electrical transport properties. Addition of CNTs enhanced the flux pinning and improved the grain boundaries of high-temperature superconductors. The effect of CNTs on other cuprate high-temperature superconductors has also been compared with these $\text{NdBa}_2\text{Cu}_3\text{O}_{7-\delta}$ samples.

Keywords Critical current density · Carbon nanoparticles · Transition temperature

1 Introduction

High-temperature superconductors (HTS) have highly anisotropic layers in their structures and their critical current density, J_c depends on their microstructural properties such as the grain boundaries and inter-grains connectivity. Many researchers studied the enhancement of J_c via various methods including substitution or addition of various nanomaterials which is one of the most practical methods due to its simplicity of implementation. Addition of nanomaterials improves the electric transport properties such as the critical current density of HTS materials due to the better connection of the grain boundaries and increasing of their

flux pinning capacities [1–9]. It is found that nanomaterials occupy the voids between the grains and affect the superconductivity by strong bonding mechanisms between the grains boundaries. Such nanomaterials act as impurities without changing the structure of HTS materials [10–13].

Besides, many researchers have studied on the addition of carbon-based nanomaterials to enhance the properties of HTS, especially for its critical current density. Recently, carbon nanotubes (CNTs) have brought great interest to researchers to enhance the J_c of these HTS materials. It is found that the addition of carbon nanotubes improves the performance of $\text{YBa}_2\text{Cu}_3\text{O}_{7-\delta}$ where the critical current density was reported to increase by 10 times [14, 15]. These nanostructure phases behave as efficient trapping centers to stop the flux motion. Subsequently, J_c under applied magnetic field also increases. Without changing the structure of the materials, adding the CNT forms electrical networks between grains as shown in the scanning electron microscope (SEM) image and improves the electric transport properties between the grains [15]. CNTs can be useful in enhancing the properties of the ceramic cuprate superconductors because they have lower density and larger surface area, and larger surface-to-volume ratio [16].

✉ Tet Vui Chong
chongtetvui@gmail.com

¹ Faculty of Engineering and Quantity Surveying, INTI International University, Persiaran Perdana BBN, Putra Nilai, 71800 Nilai, Negeri Sembilan, Malaysia

² Faculty of Data Science and Information Technology, INTI International University, Persiaran Perdana BBN, Putra Nilai, 71800 Nilai, Negeri Sembilan, Malaysia

³ Department of Applied Physics, Universiti Kebangsaan Malaysia, 43600 Bangi, Selangor, Malaysia

In view of the effectiveness of CNT and results on $\text{YBa}_2\text{Cu}_3\text{O}_{7-\delta}$, in this work, we report the effect of carbon nanotubes addition on $\text{NdBa}_2\text{Cu}_3\text{O}_{7-\delta}$ (Nd123) superconductor. Nd123 is an interesting superconductor because it has a wider solidification range and higher peritectic decomposition temperature than the widely studied $\text{YBa}_2\text{Cu}_3\text{O}_{7-\delta}$ [17, 18]. The orthorhombic-tetragonal (OT) transition occurs at $\delta_{\text{OT}} \sim 0.45$ which is significantly different from $\text{YBa}_2\text{Cu}_3\text{O}_{7-\delta}$ where $\delta_{\text{OT}} \sim 0.65$. In this study, $\text{NdBa}_2\text{Cu}_3\text{O}_{7-\delta}$ bulk samples were prepared with the addition of 0.5, 1.0 and 1.5 wt% of CNTs via the solid-state reaction method. All samples were prepared under the same condition and hence, any significant variation in the result might not be due to the samples' preparation method. The X-ray powder diffraction method was used to identify the resultant phase. The microstructure was studied using a scanning electron microscope. The effects of CNTs addition on the transport critical current density in the sample were studied using standard DC four-probe and AC susceptibility measurements.

1.1 Samples and experiments

$\text{NdBa}_2\text{Cu}_3\text{O}_{7-\delta} + x$ wt% CNTs ($x=0, 0.5, 1.0, \text{ and } 1.5$) polycrystalline samples were prepared by mixing appropriate amounts of high purity ($\geq 99.99\%$) Nd_2O_3 , BaCO_3 , CuO and CNTs ($\geq 98\%$ carbon basis from Sigma Aldrich, single walled and diameter 3–5 nm) powders. The powders were weighted in stoichiometric ratio. The mixed powders were calcined in air at around 900°C for 48 h with several intermittent grindings and oven cooled. The powders were then pressed into pellets with a diameter of around 13 mm and 2 mm thickness by using 3 kPa pressure. The pellets were sintered at 900°C for another 24 h and oven cooled. The samples were then annealed in flowing O_2 at 900°C and kept at this temperature for more than 10 h under an oxygen atmosphere. The furnace temperature was decreased to 500°C with a slow ramp rate $1.5^\circ\text{C}/\text{m}$ followed by a natural furnace cool to room temperature under an oxygen atmosphere.

The phase of the samples was confirmed using the X-ray diffraction method. The CuK_α radiation using a Siemens D5000 diffractometer was employed. The microstructure and morphology were studied using a scanning electron microscope from Philips (model XL 30). The DC electrical resistance versus temperature was measured using the four-probe method. The transport critical current density was measured at 55 K (some of the samples have $T_{\text{c zero}}$ which is lower than 77 K) using the four-probe technique. Susceptibility transition temperature was performed by AC susceptometer from Cryo Industry model REF-1808-ACS. The frequency of the AC signal was 295 Hz and the applied magnetic field was $H = 5$ Oe.

2 Results and discussion

The $\text{NdBa}_2\text{Cu}_3\text{O}_{7-\delta}$ samples need oxygen flow to optimize the oxygen content to achieve the superconducting state. Powder X-ray diffraction patterns (Fig. 1) showed that all samples are single-phase with the orthorhombic structure and space group Pmmm. This showed that the addition of CNT did not change nor enter the structure of the samples. Furthermore, there was no significant correlation between the addition of CNT with the lattice parameters. Scanning electron micrographs for samples with 0.5 and 1.0% of CNT addition are shown in Fig. 2. The micrographs did not reveal any significant variation in the morphology of the samples. Grain boundaries of the samples are well-defined. The added CNTs occupied the voids between the grains of the samples and there was no variation in lattice parameters as observed from the XRD patterns.

Figure 3 shows the temperature-dependent normalized electrical resistance of these polycrystalline samples. The results showed that adding CNTs increased the onset critical temperature, $T_{\text{c onset}}$ (Table 1). Such behavior was confirmed through the AC susceptibility measurement (Fig. 4). However, the addition of CNT broadened the width of the transition temperature, ΔT ($T_{\text{c onset}} - T_{\text{c zero}}$) of the samples. We suggest that a high amount of CNTs addition is beneficial to achieve higher $T_{\text{c onset}}$ but it may also act as an impurity and reduce the complete superconducting state of the sample due to the high percentage of CNTs addition. Increasing in $T_{\text{c onset}}$ in the CNTs-added samples could also be due to the improvement of crystallinity and structure of the samples. Figure 3 also revealed the metallic normal state of the non-added $\text{NdBa}_2\text{Cu}_3\text{O}_{7-\delta}$ sample changed to semi-metallic normal state with the

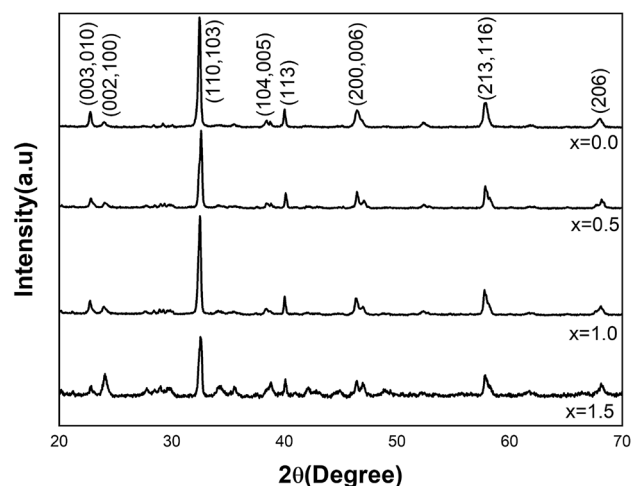


Fig. 1 X-ray powder diffraction patterns of $\text{NdBa}_2\text{Cu}_3\text{O}_{7-\delta} + x$ wt% CNTs

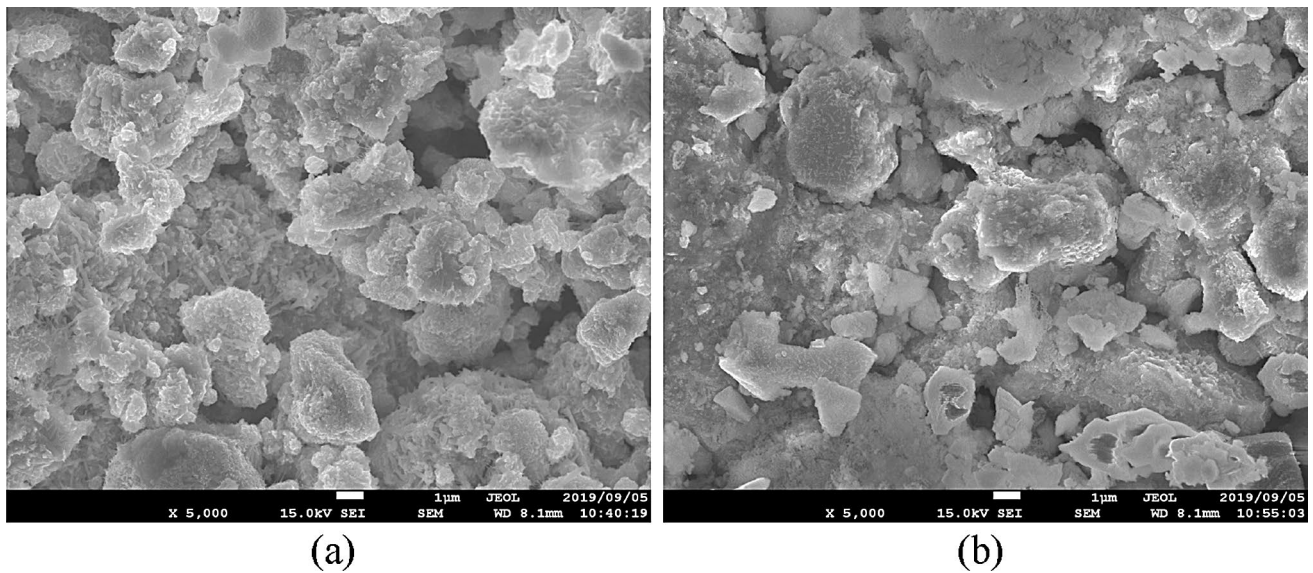


Fig. 2 Scanning electron micrograph of $\text{NdBa}_2\text{Cu}_3\text{O}_{7-\delta}$ with **a** 0.5 wt% and **b** 1.0 wt% of CNTs added sample

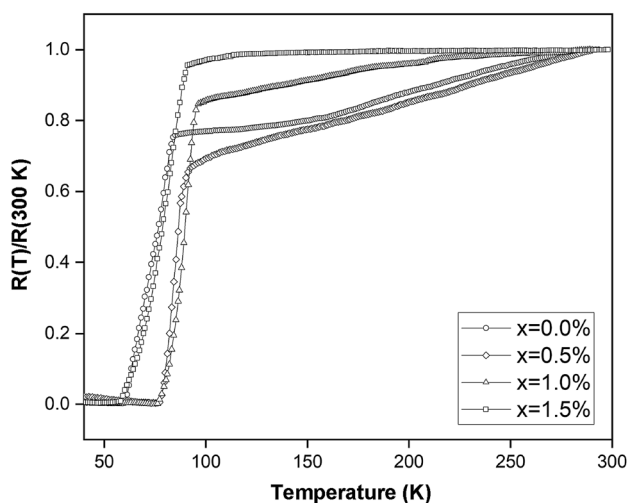


Fig. 3 Temperature-dependent electrical resistance of $\text{NdBa}_2\text{Cu}_3\text{O}_{7-\delta} + x$ wt% CNTs samples

increase of CNTs addition. This was also observed in the $\text{YBa}_2\text{Cu}_3\text{O}_{7-\delta}$ added CNTs samples [19].

It is known that the resistivity in the normal state of HTS depends on the porosity and grain boundary scattering in the samples. In this study, the normal state resistivity at room temperature increased with CNTs-added samples. It can be explained by the decrease in the relaxation time due to the greater number of defects and disorder. This is independent of the homogeneity and oxygen content in the samples since all the samples were prepared under identical condition.

The transition temperature of the samples as measured by AC susceptibility was found to be consistent with the values measured by the standard DC four-probe method (Fig. 4). The sudden drop in the real part χ' of the complex susceptibility ($\chi = \chi' + i\chi''$) was due to the diamagnetic shielding and the peak temperature, T_p in the imaginary part of the susceptibility χ'' represents AC losses. As the CNTs content was increased, the peak temperature, T_p decreased for 0.5 and 1.0

Table 1 Zero-resistance transition temperature ($T_{c\text{ zero}}$), onset transition temperature ($T_{c\text{ onset}}$), transition temperature ($T_{c\chi'}$) and peak temperature (T_p) as measured by the AC susceptibility, 300 K elec-

trical resistivity, lattice parameters and critical current density of $\text{NdBa}_2\text{Cu}_3\text{O}_{7-\delta} + x$ wt% CNTs samples

x (wt%)	$T_{c\text{ onset}}$ (K)	$T_{c\text{ zero}}$ (K)	$T_{c\chi'}$ (K)	T_p (K)	ρ (300 K) (m Ω cm)	Lattice parameters			J_c at 55 K (mA/cm 2)
						a (\AA)	b (\AA)	c (\AA)	
0.0	85	60	86	83	4.87	3.8640	3.9160	11.7490	2600
0.5	92	77	92	75	5.51	3.8740	3.9186	11.7486	3820
1.0	96	76	96	76	6.36	3.8610	3.9178	11.7320	4960
1.5	91	58	92	82	6.32	3.8897	3.9113	11.7268	4630

The uncertainty in the transition temperatures is ± 1 K

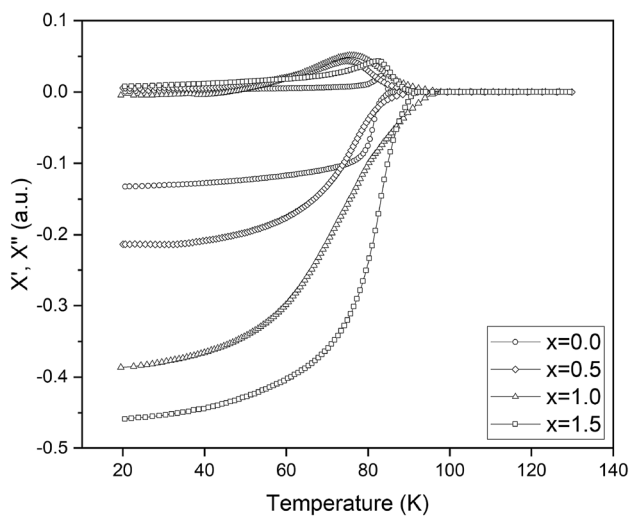


Fig. 4 Temperature-dependent AC susceptibility of $\text{NdBa}_2\text{Cu}_3\text{O}_{7-x}$ + x wt% CNTs samples

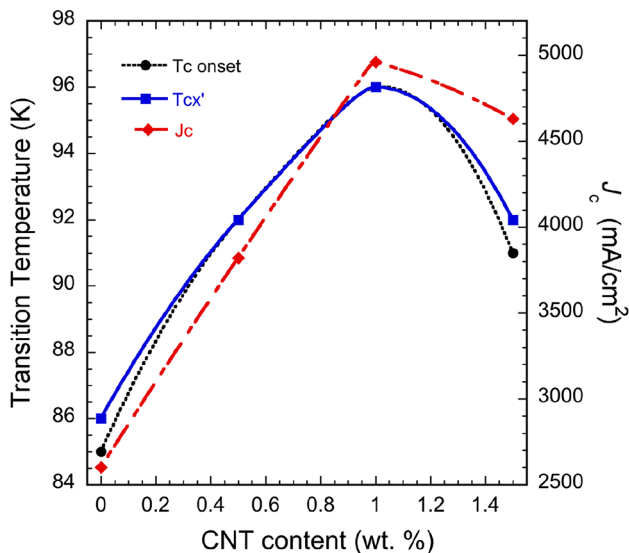


Fig. 5 $T_{c \text{ onset}}$, $T_{c\chi'}$ and J_c versus CNTs content

wt% addition. However, with further addition (1.5 wt%) T_p increased to 82 K (Fig. 4). Changes in the peak temperature indicated that the pinning force was interrupted.

Adding 1.0 wt% CNTs, increased the critical current density (at 55 K) from 2600 mA/cm² for the non-added $\text{NdBa}_2\text{Cu}_3\text{O}_{7-\delta}$ sample to 4960 mA/cm². The increase in J_c may be due to the filling of the voids by CNTs, which improved the electrical contacts between the grains. This is similar to the CNTs added $\text{YBa}_2\text{Cu}_3\text{O}_{7-\delta}$ samples where J_c increased significantly [14, 15, 19]. However, further addition (1.5 wt%) of CNTs in our Nd123 samples showed a decrease in J_c . The changes in $T_{c \text{ onset}}$, $T_{c\chi'}$ and J_c with CNTs contents are shown in Fig. 5. It can be seen that all three parameters showed the maximum value for the sample that was added with 1.0 wt% CNTs. Table 2 shows the variation of T_c with various wt% of CNTs addition in some HTS samples.

3 Conclusions

In this work, we found that adding CNTs, increased both the transition temperature and critical current density of $\text{NdBa}_2\text{Cu}_3\text{O}_{7-\delta}$ for up to 1.0 wt%. The normal state changes from metallic to semi-metallic as the amount of CNTs increases. Although the non-added $\text{NdBa}_2\text{Cu}_3\text{O}_{7-\delta}$ showed the lowest normal state resistivity (highest carrier concentration) at 300 K, it did not show the highest transition temperature and critical current density. 1.0 wt% of CNTs was observed as the optimum amount for the highest T_c and J_c . This work showed that CNTs with judicious amount can act as effective flux pinning centers and strengthen the connection of the grains boundaries which led to the higher J_c . In view of the pronounced enhancement of J_c in the $\text{NdBa}_2\text{Cu}_3\text{O}_{7-\delta}$ material, adding CNTs in other $\text{RBa}_2\text{Cu}_3\text{O}_{7-\delta}$ type phase superconductors and other cuprate-based superconductors are suggested for future works.

Table 2 Zero-resistance transition temperature ($T_{c\text{ zero}}$) and onset transition temperature ($T_{c\text{ onset}}$) of various HTS + x wt% CNTs samples

HTS	wt% CNT	$T_{c\text{ onset}}$ (K)	$T_{c\text{ zero}}$ (K)	Ref.
NdBa ₂ Cu ₃ O _{7-δ}	1.0	96	76	This work
CuTl1223 + CNT	4.0	–	–	[20]
CuTl1223 + CNT	0	112	102	[16]
	1.0	109	101	
	7.0	111	97	
GdBa ₂ Cu ₃ O _{7-δ} + SWCNT	0	89.89	76.75	[21]
	0.06	94.6	90.5	
GdBa ₂ Cu ₃ O _{7-δ} + MWCNT	0.08	93.25	87.78	
YBa ₂ Cu ₃ O _{7-δ} + CNT	0	95.3	91.4	[22]
	0.1	95.5	91.7	
	1.0	95.4	82.0	
MgB ₂ + CNT	3	30.2	–	[23]
	0	41.65	39.31	[24]

Acknowledgements This work was supported by INTI IU under Seeding Grant no. INT-FITS-03-01-2017 and the Ministry of Higher Education, Malaysia under Grant number FRGS/1/2020/STG07/UKM/01/1.

Author contributions TVC conceptualization, resources, writing—original draft, supervision, writing—review and editing; SKL methodology, investigation, validation, formal analysis; CHL methodology, investigation, validation, formal analysis; RA-S funding acquisition, writing—original draft, writing—review and editing.

Declarations

Conflict of interest The authors declare that they have no known competing financial interests or personal relationships that could have appeared to influence the work reported in this paper.

Open Access This article is licensed under a Creative Commons Attribution 4.0 International License, which permits use, sharing, adaptation, distribution and reproduction in any medium or format, as long as you give appropriate credit to the original author(s) and the source, provide a link to the Creative Commons licence, and indicate if changes were made. The images or other third party material in this article are included in the article's Creative Commons licence, unless indicated otherwise in a credit line to the material. If material is not included in the article's Creative Commons licence and your intended use is not permitted by statutory regulation or exceeds the permitted use, you will need to obtain permission directly from the copyright holder. To view a copy of this licence, visit <http://creativecommons.org/licenses/by/4.0/>.

References

- M.K. Ben Salem, E. Hannachi, Y. Slimani, A. Hamrita, M. Zouaoui, L. Bessais, M. Ben Salem, F. Ben Azzouz, SiO₂ nanoparticles addition effect on microstructure and pinning properties in YBa₂Cu₃O _{y} . *Ceram. Int.* **40**, 4953–4962 (2014)
- S. Dadras, Z. Gharehgasloo, Effect of Au nano-particles doping on polycrystalline YBCO high temperature superconductor. *Phys. B.* **492**, 45–49 (2016)
- A.A. Khan, M. Mumtaz, M. Khan, L. Ali, M. Rahim, M. Ali, Effects of non-magnetic metallic zinc nanoparticles on the dielectric properties of CuTl-1223 superconducting phase. *J. Supercond. Nov. Magn.* **34**, 1341–1350 (2021)
- A. Bahboh, A.H. Shaari, H. Baqiah, S.K. Chen, M.M.A. Kechik, M.H. Wahid, R. Abd-Shukor, Z.A. Talib, Effects of HoMnO₃ nanoparticles addition on microstructural, superconducting and dielectric properties of YBa₂Cu₃O_{7- δ} . *Ceram. Int.* **45**, 13732–13739 (2019)
- R. Algarni, M.A. Almessiere, Y. Slimani, E. Hannachi, F. Ben Azzouz, Enhanced critical current density and flux pinning traits with Dy₂O₃ nanoparticles added to YBa₂Cu₃O_{7- δ} superconductor. *J. Alloy. Compd.* **852**, 157019 (2021)
- M. Dahiya, R. Kumar, D. Kumar, D. Kumar, N. Khare, Investigation of the flux pinning properties of YBCO/NaNbO₃ nanoparticle composite superconductor. *J. Supercond. Nov. Magn.* **34**, 2249–2257 (2021)
- Y. Slimani, M.A. Almessiere, E. Hannachi, A. Manikandan, R. Algarni, A. Baykal, F. Ben Azzouz, Flux pinning properties of YBCO added by WO₃ nanoparticles. *J. Alloy. Compd.* **810**, 151884 (2019)
- Y. Slimani, E. Hannachi, M. Zouaoui, F. Ben Azzouz, M. Ben Salem, Excess conductivity investigation of Y₃Ba₅Cu₈O_{18 \pm δ} superconductors prepared by various parameters of planetary ball milling technique. *J. Supercond. Nov. Magn.* **31**(8), 2339–2348 (2018)
- E. Hannachi, Y. Slimani, A. Ekicibil, A. Manikandan, F. Ben Azzouz, Magneto-resistivity and magnetization investigations of YBCO superconductor added by nano-wires and nano-particles of titanium oxide. *J. Mater. Sci. Mater. Electron.* **30**(9), 8805–8813 (2019)
- G.E. Jang, W.S. Oh, C.J. Kim, Y.H. Han, S.Y. Jung, T.H. Sung, The effect of impregnation by resin and CNT compound on the mechanical and magnetic properties of YBCO superconductor. *Physica. C.* **468**, 1411–1414 (2008)
- M.Z. Shoushtari, M. Akbari, Y. Hajati, Study of YBa₂Cu₃O_{7- δ} superconductor/graphene oxide composite. *J. Supercond. Nov. Magn.* **31**, 2733–2739 (2018)
- S.X. Dou, S. Soltanian, J. Horvat, X.L. Wang, S.H. Zhou, M. Ionescu, H.K. Liu, Enhancement of the critical current density and flux pinning of MgB₂ superconductor by nanoparticle SiC doping. *Appl. Phys. Lett.* **81**, 3419 (2002)
- W.X. Li, Y. Li, R.H. Chen, W.K. Yoeh, S.X. Dou, Effect of magnetic field processing on the microstructure of carbon nanotubes doped MgB₂. *Phys. C.* **460–462**, 570–571 (2007)

14. E. Hannachi, M.A. Almessiere, Y. Slimani, A. Baykal, F. Ben Azzouz, AC susceptibility investigation of YBCO superconductor added by carbon nanotubes. *J. Alloy. Compd.* **812**, 152150 (2020)
15. S. Dadras, Y. Liu, Y.S. Chai, V. Daadmehr, K.H. Kim, Increase of critical current density with doping carbon nano-tubes in $\text{YBa}_2\text{Cu}_3\text{O}_{7-\delta}$. *Phys. C.* **469**(1), 55–59 (2009)
16. N.A. Khan, S. Aziz, Single and multi-walled carbon nanotubes doped $(\text{Cu}_{0.5}\text{Tl}_{0.5})\text{Ba}_2\text{Ca}_2\text{Cu}_3\text{O}_{10-\delta}$ superconductors. *J. Alloy. Compd.* **538**, 183–188 (2012)
17. K. Oka, M. Saito, M. Ito, K. Nakane, K. Murata, Y. Nishihara, H. Unoki, Phase Diagram and crystal growth of $\text{NdBa}_2\text{Cu}_3\text{O}_{7-y}$. *Jpn. J. Appl. Phys.* **28**, L219 (1989)
18. J. Ullmann, R.W. Mccallum, J.D. Verhoeven, Effect of atmosphere and rare earth on liquidus relations in RE–Ba–Cu oxides. *J. Mater. Res.* **4**, 752–754 (1989)
19. N.A. Khalid, M.M.A. Kechik, N.A. Baharuddin, S.K. Chen, H. Baqiah, N.N.M. Yusuf, A.H. Shaari, A. Hashim, Z.A. Talib, Impact of carbon nanotubes addition on transport and superconducting properties of $\text{YBa}_2\text{Cu}_3\text{O}_{7-\delta}$ ceramics. *Ceram. Int.* **44**(8), 9568–9573 (2018)
20. M.A. Rafique, S. Aziz, N. Hassan, N.A. Khan, Enhanced magnetic properties in $\text{Cu}_{0.5}\text{Tl}_{0.5}\text{Ba}_2\text{Ca}_2\text{Cu}_3\text{O}_{10-\delta}$ superconductor doped with carbon nanotubes. *J. Supercond. Nov. Magn.* **27**, 2427–2434 (2014)
21. A.I. Abou-Aly, M. Anas, S. Ebrahimi, R. Awad, I.G. Eldeenz, Comparative studies between the influence of single- and multi-walled carbon nanotubes addition on Gd-123 superconducting phase. *Mod. Phys. Lett. B* **30**(36), 1650418 (2016)
22. E. Hannachi, M.A. Almessiere, Y. Slimani, R.B. Alshamrani, G. Yasin, F. Ben Azzouz, Preparation and characterization of high- T_c $(\text{YBa}_2\text{Cu}_3\text{O}_{7-\delta})_{1-x}/(\text{CNTs})_x$ superconductors with highly boosted superconducting performances. *Ceram. Int.* **47**(16), 23539–23548 (2021)
23. Y. Zhao, Y. Yang, C.H. Cheng, Y. Zhang, Doping and effect of nano-diamond and carbon-nanotubes on flux pinning properties of MgB_2 . *Phys. C.* **463–465**, 165–169 (2007)
24. S.D. Yudanto, Y.P. Dewi, P. Sebayang, S.A. Chandra, A. Imaduddin, B. Kurniawan, A. Manaf, Influence of CNTs addition on structural and superconducting properties of mechanically alloyed MgB_2 . *J. Met. Mater. Miner.* **30**(3), 9–14 (2020)

Publisher's Note Springer Nature remains neutral with regard to jurisdictional claims in published maps and institutional affiliations.